

AD-A037 371

TEXAS UNIV AT AUSTIN APPLIED RESEARCH LABS
QUARTERLY PROGRESS REPORT FOR JULY, AUGUST, AND SEPTEMBER 1970. (U)
OCT 70

N00024-70-C-1279

NL

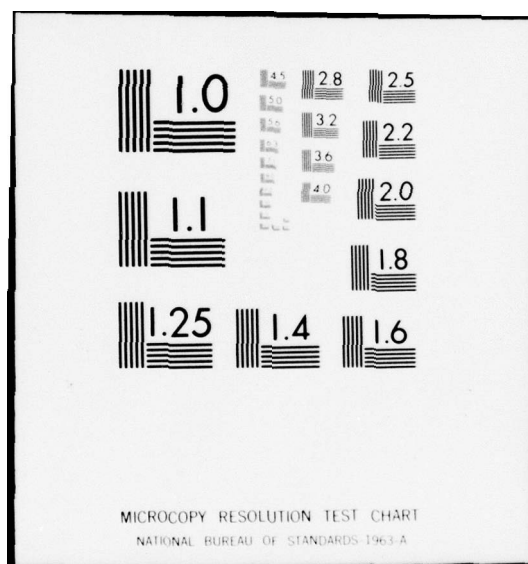
UNCLASSIFIED

1 OF 1
ADA037371



END

DATE
FILMED
4-77



Good
MOST Project -2

ADA037371

APPLIED
RESEARCH
LABORATORIES

THE UNIVERSITY OF TEXAS
AT AUSTIN

8 October 1970

Copy No. 1

QUARTERLY PROGRESS REPORT
UNDER CONTRACT N00024-70-C-1279
FOR JULY, AUGUST, AND SEPTEMBER 1970

NAVAL SHIP SYSTEMS COMMAND
Contract N00024-70-C-1279
Proj. Ser. No. SF 11552-001, Task 8118

DDC FILE COPY,

000892

Ge. x

*See Form
1473*



DDC
RECEIVED
MAR 8 1977
D

DISTRIBUTION STATEMENT A

Approved for public release;
Distribution Unlimited

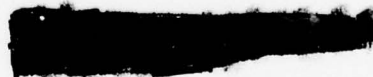
701112-0059

8 October 1970

QUARTERLY PROGRESS REPORT
UNDER CONTRACT N00024-70-C-1279
FOR JULY, AUGUST, AND SEPTEMBER 1970

NAVAL SHIP SYSTEMS COMMAND
Contract N00024-70-C-1279
Proj. Ser. No. SF 11552-001, Task 8118

ADDITIONAL	
White Section	<input checked="" type="checkbox"/>
Buff Section	<input type="checkbox"/>
Blank Section	<input type="checkbox"/>
Per Hq. on file	
SECURITY CODES	
A	



DDC
RECEIVED
MAR 8 1977
D

APPLIED RESEARCH LABORATORIES
THE UNIVERSITY OF TEXAS AT AUSTIN
AUSTIN, TEXAS 78712

DISTRIBUTION STATEMENT A
Approved for public release;
Distribution Unlimited

1112-0059
404 134

ABSTRACT

In Section I the Rayleigh reflection coefficient for a rough surface is derived in a form suitable for inclusion in the basic integral for the scattered pressure. A formula for the pressure scattered from a rough attenuating surface is then derived using this coefficient. The backscattered intensity is calculated in Section II for various assumed distributions of surface heights. The results presented here are restricted to the high frequency limit, and are developed using both the stationary phase and the modified Fresnel techniques. Finally, a backscattering result for a composite surface is derived, and is shown to be consistent for both forward and backward scattering.

TABLE OF CONTENTS

	<u>Page</u>
ABSTRACT	iii
I. SCATTERED PRESSURE FROM A RANDOMLY ROUGH ATTENUATING SURFACE	1
II. BACKSCATTERING THEORY AND EXPERIMENT	13
A. Introduction	13
B. Stationary Phase Backscatter	14
C. Fresnel High Frequency Backscatter	17
1. Gaussian Bivariate Distribution	23
2. Exponential Bivariate Distribution	24
3. Three-halves Bivariate Distribution	25
D. Composite Surface Theory	31
REFERENCES	37

1. SCATTERED PRESSURE FROM A RANDOMLY ROUGH ATTENUATING SURFACE

During this quarter it was discovered that the expressions given in the previous progress report for the Rayleigh reflection coefficient for a rough surface were inadequate. The results given previously were only approximate due to an error in the method in which Snell's law was applied to the coefficient. This quarter a more complete and accurate treatment of this problem was derived. The following derivation differs from the original treatment of the problem not only in the form of the Rayleigh coefficient itself, but also in that the coefficient is used in the context of the original integral for the scattered pressure.

The scattered pressure at point A is given by the integral

$$p_s(A) = \frac{1}{2\pi} \iint_{\Sigma} p_s(N) \frac{\partial}{\partial n} \left(\frac{e^{ikr_1}}{r_1} \right) ds, \quad (1)$$

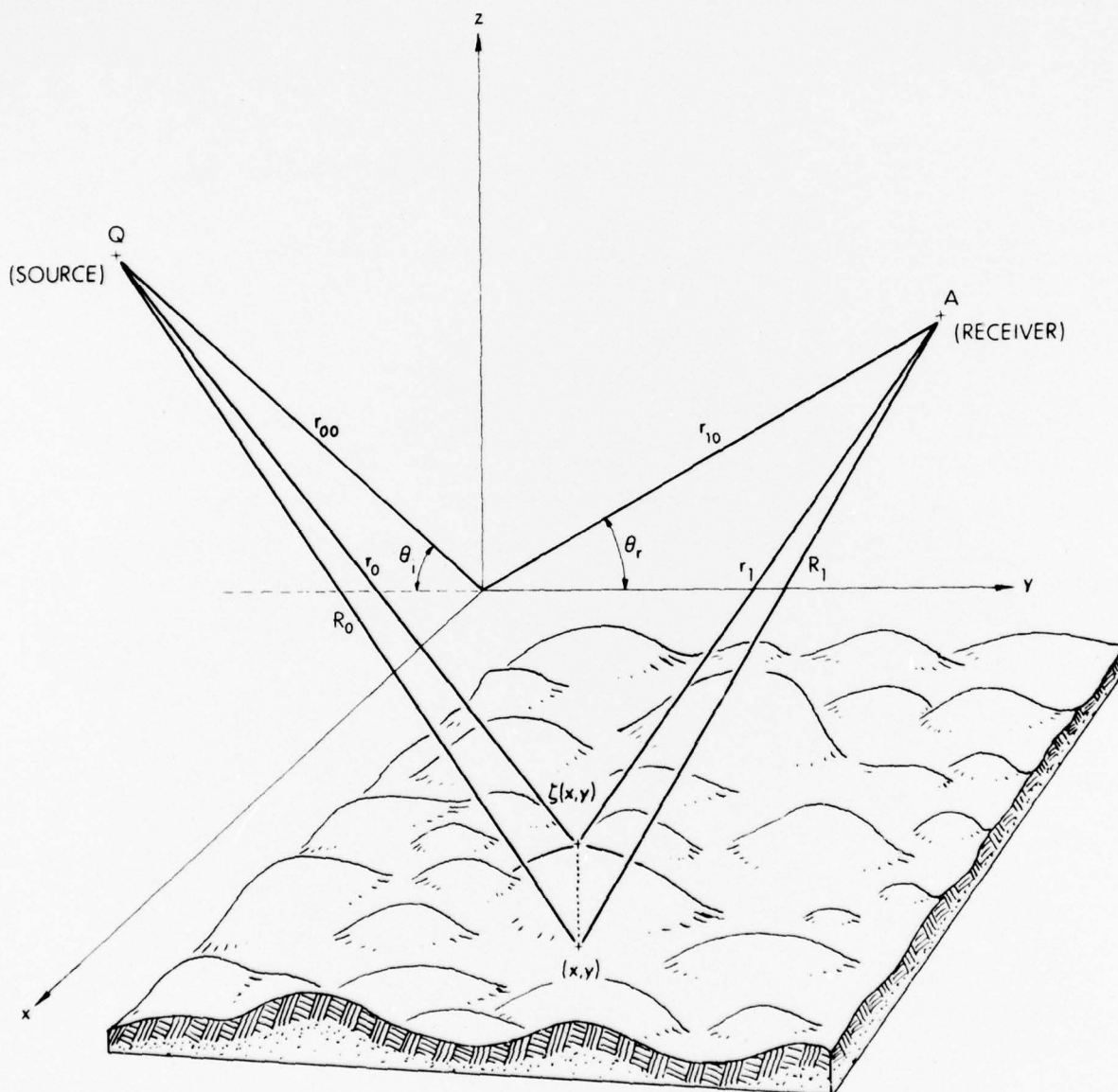
where

N is a variable point on the surface,

n is the outward normal to the surface, and

r_1 is defined in Dwg. AS-68-1100. The exact form of the Kirchhoff boundary condition is

$$\frac{p_s(N)}{p_i} = R, \quad (2)$$



SCATTERING GEOMETRY

where $p_s(N)$ and p_i are the values of the scattered and incident pressures on the surface and R is the Rayleigh reflection coefficient which will later be shown to be a function of the local slope of the surface. If it is now assumed that the incident pressure is of the form

$$p_i = P_o \frac{e^{ikr_o}}{r_o} , \quad (3)$$

it is then obvious that

$$p_s(N) = RP_o \frac{e^{ikr_o}}{r_o} , \quad (4)$$

and

$$p_s(A) = \frac{1}{2\pi} \iint_{\Sigma} RP_o \left(\frac{e^{ikr_o}}{r_o} \right) \frac{\partial}{\partial n} \left(\frac{e^{ikr_l}}{r_l} \right) ds . \quad (5)$$

Following the development given in Section III - D of the Final Report under Contract N00024-69-C-1275, this integral becomes

$$p_s(A) = \frac{ik}{2\pi} \iint_{\Sigma} P_o R \left(\frac{e^{ik(R_o+R_l)}}{R_o R_l} \right) e^{-iky\zeta} \left(\zeta_x \hat{e}_x + \zeta_y \hat{e}_y - \hat{e}_z \right) \cdot \hat{e}_l \, dx dy , \quad (6)$$

where

$$\gamma = \sin\theta_l + \sin\theta_r , \quad (7)$$

and \hat{e}_1 is a unit vector directed along line R_1 . Continuing this derivation, it is now assumed that

$$\begin{aligned}\hat{e}_x \cdot \hat{e}_1 &= 0, \\ \hat{e}_y \cdot \hat{e}_1 &= \cos\theta_r, \\ \hat{e}_z \cdot \hat{e}_1 &= \sin\theta_r,\end{aligned}\tag{8}$$

so that

$$(\zeta_x \hat{e}_x + \zeta_y \hat{e}_y - \hat{e}_z) \cdot \hat{e}_1 = -\sin\theta_r + \zeta_y \cos\theta_r.\tag{9}$$

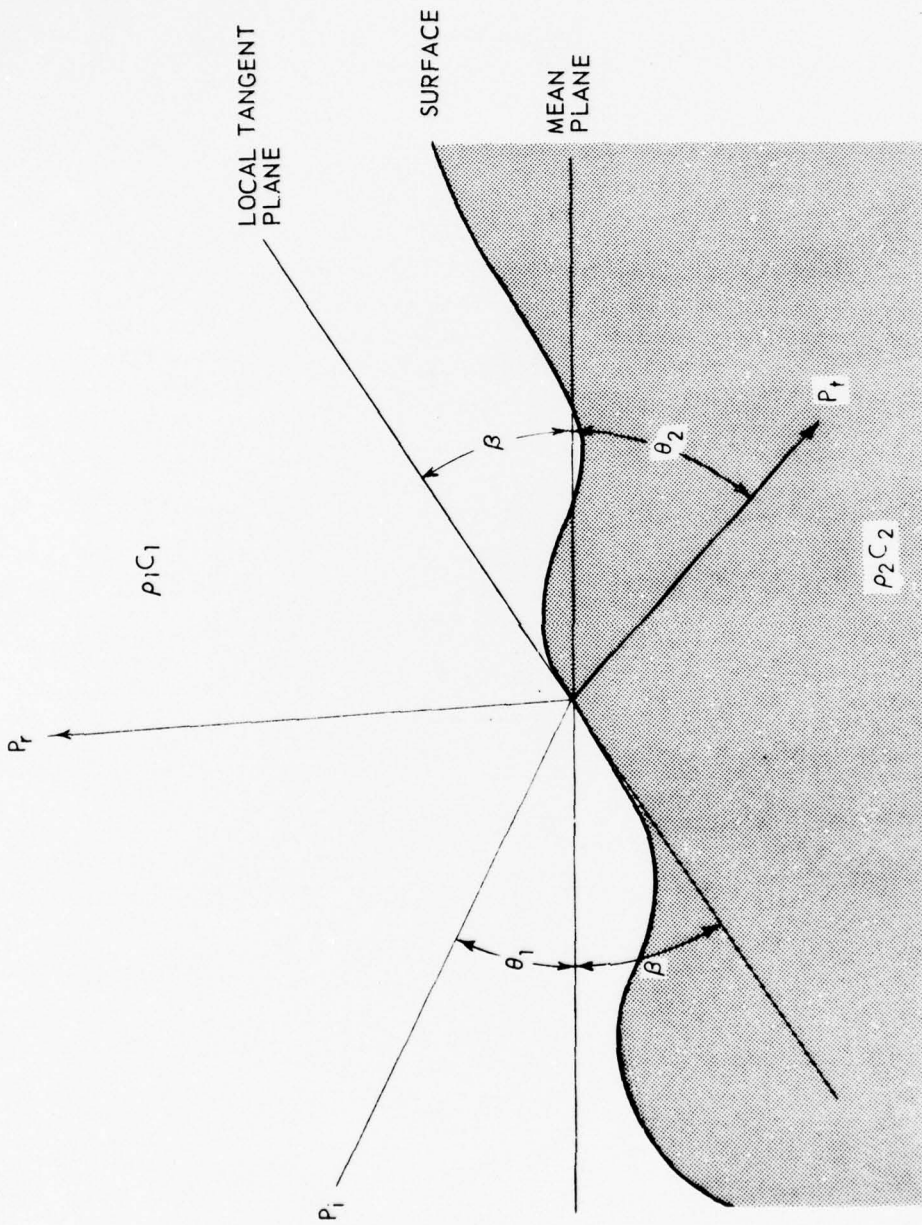
Thus the integral for the scattered pressure is

$$p_s(A) = \frac{ik}{2\pi} \iint_{\Sigma} P_o \left(\frac{e^{ik(R_o + R_1)}}{R_o R_1} \right) e^{-iky\zeta} \left[R(-\sin\theta_r + \zeta_y \cos\theta_r) \right] dx dy.\tag{10}$$

Before this integral can be further simplified, a suitable expression for the Rayleigh coefficient must be derived. Referring to Dwg. AS-70-795, the Rayleigh reflection coefficient is given by

$$R(\phi_1, \phi_2) = \frac{\rho_2 c_2 \sin\phi_1 - \rho_1 c_1 \sin\phi_2}{\rho_2 c_2 \sin\phi_1 + \rho_1 c_1 \sin\phi_2},\tag{11}$$

$$\text{where } \phi_1 = \theta_1 + \beta \text{ and } \phi_2 = \theta_2 + \beta.\tag{12}$$



PENETRABLE ROUGH SURFACE GEOMETRY

At this point Snell's law must be applied to the formula by making the substitution

$$\sin\phi_2 = \sqrt{1 - \cos^2\phi_2} = \frac{1}{N} \sqrt{N^2 - \cos^2\phi_1} \quad , \quad (13)$$

where N is the acoustic index of refraction. Applying Eq. (12) and Eq. (13) to Eq. (11) gives

$$R(\theta_1 + \beta) = \frac{\rho_2 c_2 \sin(\theta_1 + \beta) - \frac{\rho_1 c_1}{N} \sqrt{N^2 - \cos^2(\theta_1 + \beta)}}{\rho_2 c_2 \sin(\theta_1 + \beta) + \frac{\rho_1 c_1}{N} \sqrt{N^2 - \cos^2(\theta_1 + \beta)}} \quad . \quad (14)$$

By expanding $\sin(\theta_1 + \beta)$ and $\cos(\theta_1 + \beta)$ and using various trigonometric identities, this may be arranged into the form

$$R(\theta_1, \eta) = \frac{A + B\eta - C\sqrt{D\eta^2 + E\eta + F}}{A + B\eta + C\sqrt{D\eta^2 + E\eta + F}} \quad , \quad (15)$$

where

$$\eta = \tan\beta \quad , \quad \text{and} \quad (16)$$

$$A = \rho_2 c_2 \sin\theta_1 \quad ,$$

$$B = \rho_2 c_2 \cos\theta_1 \quad ,$$

$$C = \frac{\rho_1 c_1}{N} \quad , \quad (17)$$

$$D = N^2 - \sin^2\theta_1 \quad ,$$

$$E = \sin^2\theta_1 \quad ,$$

$$F = N^2 - \cos^2\theta_1 \quad .$$

For ease of application, $R(\theta_1, \eta)$ is expanded in a Maclaurin series:

$$R(\theta_1, \eta) = R|_{\eta=0} + \left. \frac{\partial R}{\partial \eta} \right|_{\eta=0} \eta + \left. \frac{\partial^2 R}{\partial \eta^2} \right|_{\eta=0} \frac{\eta^2}{2!} + \dots, \quad (18)$$

where

$$R|_{\eta=0} = \frac{A - C\sqrt{F}}{A + C\sqrt{F}} = \frac{\rho_2 c_2 \sin \theta_1 - \frac{\rho_1 c_1}{N} \sqrt{N^2 - \cos^2 \theta_1}}{\rho_2 c_2 \sin \theta_1 + \frac{\rho_1 c_1}{N} \sqrt{N^2 - \cos^2 \theta_1}}, \quad (19)$$

$$\left. \frac{\partial R}{\partial \eta} \right|_{\eta=0} = \frac{2C \left(B\sqrt{F} - \frac{AE}{2\sqrt{F}} \right)}{(A + C\sqrt{F})^2}, \quad (20)$$

$$\left. \frac{\partial^2 R}{\partial \eta^2} \right|_{\eta=0} = \frac{\left[A + C\sqrt{F} \right] \left[\frac{2BCE - 2AD - BE}{2\sqrt{F}} \right] - 4C \left[B\sqrt{F} - \frac{AE}{2\sqrt{F}} \right] \left[B + \frac{CE}{2\sqrt{F}} \right]}{(A + C\sqrt{F})^3}. \quad (21)$$

The first term of this series is just the Rayleigh reflection coefficient for a plane surface.

Since η is the tangent of β , it is obvious from Dwg. AS-70-795 that η is just the slope of the local tangent. Because the formulation is restricted to the plane of incidence, it may be assumed that $\eta = \zeta y$. Using this in the original pressure integral gives

$$p_s(A) = \frac{ik}{2\pi} \iint_{\Sigma} P_o \left(\frac{e^{ik(R_o + R_1)}}{R_o R_1} \right) e^{-ik\eta \zeta} \left[R(\theta_1, \eta) (-\sin \theta_r + \eta \cos \theta_r) \right] dx dy. \quad (22)$$

At this point ζ and η are recognized as random variables and the integral for $p_s(A)$ must be replaced by $\langle p_s(A) \rangle$. If it is assumed that the surface height, ζ , and the surface slope, η , are independent, then the integral for $\langle p_s(A) \rangle$ takes on the simple form

$$\langle p_s(A) \rangle = \frac{ik}{2\pi} \iint_{\Sigma} P_o \left(\frac{e^{ik(R_o + R_1)}}{R_o R_1} \right) \langle e^{ik\gamma\zeta} \rangle \langle R(\theta_1, \eta) (-\sin\theta_r + \eta \cos\theta_r) \rangle dx dy \quad (23)$$

Since it has been assumed that η is stationary and independent of ζ , it may be shown that

$$\begin{aligned} \langle p_s(A) \rangle &= \langle R(\theta_1, \eta) (1 - \eta \cot\theta_r) \rangle \left(\frac{-ik}{2\pi} \right) \iint_{\Sigma} P_o \sin\theta_r \left(\frac{e^{ik(R_o + R_1)}}{R_o R_1} \right) \\ &\quad \cdot \langle e^{ik\gamma\zeta} \rangle dx dy \quad (24) \end{aligned}$$

Since ζ is also stationary, its expectation value may also be removed from the integral, leaving only a form which is immediately recognized as the pressure scattered from a plane surface.

$$\langle p_s(A) \rangle = \left[\langle R(\theta_1, \eta) \rangle - \cot\theta_r \langle \eta R(\theta_1, \eta) \rangle \right] \langle e^{-ik\gamma\zeta} \rangle p_r \quad (25)$$

Assuming a Gaussian distribution of heights,

$$\langle p_s(A) \rangle = \left[\langle R(\theta_1, \eta) \rangle - \cot\theta_r \langle \eta R(\theta_1, \eta) \rangle \right] e^{-\frac{g}{2}} p_r \quad , \quad 26$$

where

$$g = (k\gamma\sigma)^2,$$

θ_r is the receiver angle, and

p_r is the pressure scattered from a plane surface.

This form is particularly simple to calculate due to the form of the expansion of $R(\theta_1, \eta)$. Rearranging terms of the series gives

$$\begin{aligned} \left[\langle R \rangle - \cot\theta_r \langle \eta R \rangle \right] &= \left[R(1 - \langle \eta \rangle \cot\theta_r) + R'(\langle \eta \rangle - \langle \eta^2 \rangle \cot\theta_r) \right. \\ &\quad \left. + \frac{R''}{2} (\langle \eta^2 \rangle - \langle \eta^3 \rangle \cot\theta_r) + \dots \right] \end{aligned} \quad (27)$$

Thus the only expectation values to be calculated are of the form

$$\langle \eta^l \rangle = \int_{-\tan\theta_1}^{\infty} \eta^l P(\eta) d\eta, \quad (28)$$

where the lower limit of $-\tan\theta_1$ represents a simple shadowing consideration. For the Gaussian case these integrals are quite easy to calculate and become

$$\langle \eta^l \rangle = \frac{1}{\sqrt{2\pi}s} \int_{-\tan\theta_1}^{\infty} \eta^l e^{-\frac{\eta^2}{2s^2}} d\eta, \quad (29)$$

where s is the rms slope of the unshadowed surface.

For the case where l is an odd integer, this becomes

$$\langle \eta^l \rangle = \frac{1}{\sqrt{2\pi s}} \int_{\tan\theta_1}^{\infty} \eta^l e^{-\frac{\eta^2}{2s^2}} d\eta \quad . \quad (30)$$

Now let

$$\xi = \eta^2 \quad , \quad d\xi = 2\eta d\eta \quad , \quad (31)$$

so that

$$\langle \eta^l \rangle = \frac{1}{2\sqrt{2\pi s}} \int_{\tan^2\theta_1}^{\infty} \xi^{\frac{l-1}{2}} e^{-\frac{\xi}{2s^2}} d\xi \quad . \quad (32)$$

This may be easily integrated using Gradshteyn and Ryzhik integral No. 3.381-3 (p. 317, 4th edition) and is found to be

$$\langle \eta^l \rangle = \frac{1}{2\sqrt{2\pi s}} \left(\frac{1}{2s^2} \right)^{-\left(\frac{l+1}{2}\right)} \Gamma\left(\frac{l+1}{2}, \frac{\tan^2\theta_1}{2s^2}\right) \quad , \quad (33)$$

where $\Gamma(a, x)$ is the incomplete gamma function.

For the case where l is an even integer

$$\langle \eta^l \rangle = 2 \int_0^{\tan\theta_1} \eta^l P(\eta) d\eta + \int_{\tan\theta_1}^{\infty} \eta^l P(\eta) d\eta \quad . \quad (34)$$

Proceeding in a similar manner this gives

$$\langle \eta^\ell \rangle = \frac{1}{2\sqrt{2\pi s}} \left(\frac{1}{2s^2} \right)^{-\left(\frac{\ell+1}{2}\right)} \left[\Gamma\left(\frac{\ell+1}{2}, \frac{\tan^2 \theta_1}{2s^2}\right) + 2\gamma\left(\frac{\ell+1}{2}, \frac{\tan^2 \theta_1}{2s^2}\right) \right] \quad (35)$$

These values may be easily calculated and combined with the values of R , $\left. \frac{\partial R}{\partial \eta} \right|_{\eta=0}$, $\left. \frac{\partial^2 R}{\partial \eta^2} \right|_{\eta=0}$, etc., to find the value of $\left[\langle R \rangle - \cot \theta_r \langle \eta R \rangle \right]$.

The values of R , R' , and R'' will be complex because of the assumed attenuation in the bottom, so the entire expression for the pressure will also be complex. An initial numerical calculation was made using only the first two terms of the expansion of $R(\theta_1, \eta)$ which gave a reasonable agreement with Mackenzie's theoretical curves, which were presented in the previous progress report. However, the lack of agreement in certain areas of the curves indicates the need to include higher order terms in the calculation.

II. BACKSCATTERING THEORY AND EXPERIMENT

A. Introduction

The analysis of experimental backscattering data proves much more difficult than analysis of either forward or specular scattering data. Many investigators have assumed a composite (several types of independent irregularities) scattering mechanism in order to obtain the desired fit to their experimental data. However, if the same composite theory (with the same input parameters) is applied to forward scattering predictions, satisfactory agreements are not obtained. In addition, many composite treatments are limited to use of the nonanalytic exponential correlation function. In Section D of this chapter a qualitative description of a composite theory (two types of roughness in this case) is given which does not have these limitations. However, the assumption of two types of irregularities requires that the surface statistics be known in great detail. In fact, it is difficult to see how the composite assumption is going to help the backscattering prediction problem other than to provide an "adjustable" parameter.

Section B will be devoted to an alternate method which yields final results similar to those obtained by the composite approach by using an exponential correlation function. The method used will be the stationary phase technique developed in the Final Report under Contract N00024-69-C-1275. The stationary phase equations yield good agreement with the forward and specular scattering data.

B. Stationary Phase Backscatter

The basic formula for the stationary phase method is taken as Eq. (49) from the Final Report under Contract N00024-69-C-1275. Equation (49) states that the scattering coefficient σ (not the scattering strength) can be written as follows:

$$\sigma = \frac{\langle I_s \rangle}{I_p}$$

$$= \rho^2 \langle e^{-ik\gamma\zeta} \rangle^2 + \frac{AF^2(r_{oo} + r_{lo})^2}{\gamma^2 r_{oo}^2 r_{lo}^2} \left\{ \frac{k^2 \gamma^2}{2\pi} \int_0^\infty J_0(V_{xy} r) \langle e^{-ik\gamma(\zeta - \zeta')} \rangle \right\} r dr$$

$$\times \left[1 - \rho^2 \langle e^{-ik\gamma\zeta} \rangle^2 \right], \quad (36)$$

where the notation and geometry are used in the previously referenced final report. Equation (36) is next integrated for the case of a three-halves distribution of heights.

The marginal probability density function for the three-halves distribution of heights is given by

$$p(\zeta) = \frac{h^2}{2(h^2 + \zeta^2)^{3/2}}, \quad (37)$$

and the bivariate distribution is given by

$$p(\zeta, \zeta') = \frac{1}{2\pi h^2 (1-C)^{1/2}} \frac{1}{\left[1 + \frac{\zeta^2 - 2\zeta\zeta'C + \zeta'^2}{h^2(1-C^2)} \right]^{3/2}} \quad (38)$$

Since a variance does not exist for these distributions, a convenient quantity to equate to the experimental rms height is given by the interquartile range. The interquartile range can be written as $\frac{2}{\sqrt{3}} h$.

The characteristic functions associated with Eq. (37) and Eq. (38) can be stated as

$$\langle e^{-ik\gamma\zeta} \rangle = k\gamma h K_1(k\gamma h) \quad (39)$$

$$\langle e^{-ik\gamma(\zeta - \zeta')} \rangle = e^{-[2g(1-C)]^{1/2}}, \quad (40)$$

where $g \equiv k^2 \gamma^2 h^2$ and $h = 0.866 h_e$ (experimental rms height).

When Eqs. (39) and (40) are used in Eq. (36) we obtain the following scattering coefficient:

$$\sigma = \rho^2 g K_1^2(g^{1/2}) + \frac{AF^2(r_{oo} + r_{lo})^2}{\gamma^2 r_{oo}^2 r_{lo}^2} \left\{ \frac{k^2 \gamma^2}{2\pi} \int_0^\infty J_0(V_{xy} r) e^{-[2g(1-C)]^{1/2}} r dr \right\} \\ \times \left[1 - \rho^2 g K_1^2(g^{1/2}) \right] \quad (41)$$

The asymptotic form of Eq. (41) can be stated as

$$\sigma_{hf} = \rho^2 g K_1^2(g^{1/2}) + \frac{AF^2(r_{oo} + r_{lo})^2}{\gamma^2 r_{oo}^2 r_{lo}^2} \left\{ \frac{k^2 \gamma^2}{2\pi} \frac{L^2}{2g \left(1 + V_{xy}^2 \frac{L^2}{2g} \right)^{3/2}} \right\} \left[1 - \rho^2 g K_1^2(g^{1/2}) \right] \quad (42)$$

where a Gaussian correlation function (with correlation length L) has been assumed. If the full series expansion for Eq. (40) is applied to Eq. (41), we obtain the following form:

$$\sigma = \rho^2 g K_1^2 (g^{1/2}) + \frac{A^2 F^2 k^2 (r_{oo} + r_{lo})^2 e^{-(2g)^{1/2}}}{2\pi r_{oo}^2 r_{lo}^2} \left(\sum_{n=1}^{\infty} \frac{1}{n!} \frac{L^2 e^{-v_{xy}^2 L^2 / 4n}}{2n} \right. \\ \left. \times \sum_{m=1}^n \sum_{j=1}^{\frac{m+1}{2}} \frac{(-1)^{j-1} (2g)^{m/2} (2n-2j-1)!!}{2^n (m-2j+1)! (j-1)! 2^{j-1}} \right) \left[1 - \rho^2 g K_1^2 (g^{1/2}) \right], \quad (43)$$

where the Gaussian correlation function again has been used. In order to compare with other authors' work, Eq. (42) can also be stated (for backscattering) as

$$\sigma_{hf} = \rho^2 g K_1^2 (g^{1/2}) + \frac{A(r_{oo} + r_{lo})^2}{r_{oo}^2 r_{lo}^2} \left\{ \frac{G}{8\pi (\cos^4 \Phi + G \sin^2 \Phi)^{3/2}} \right\} \\ \times \left[1 - \rho^2 g K_1^2 (g^{1/2}) \right], \quad (44)$$

where

$$G \equiv L^2 \cos^2 \Phi / 2h^2,$$

$$F = 1/\cos \Phi, \text{ and}$$

Φ represents the angle of incidence, (i.e., $\Phi + \theta = 90$ deg).

The expression in braces is of the same form obtained by Fung and Leovaris [Ref. 1], Beckmann [Ref. 2], and Marcus [Ref. 3]. However, these authors used the nonanalytic exponential correlation function

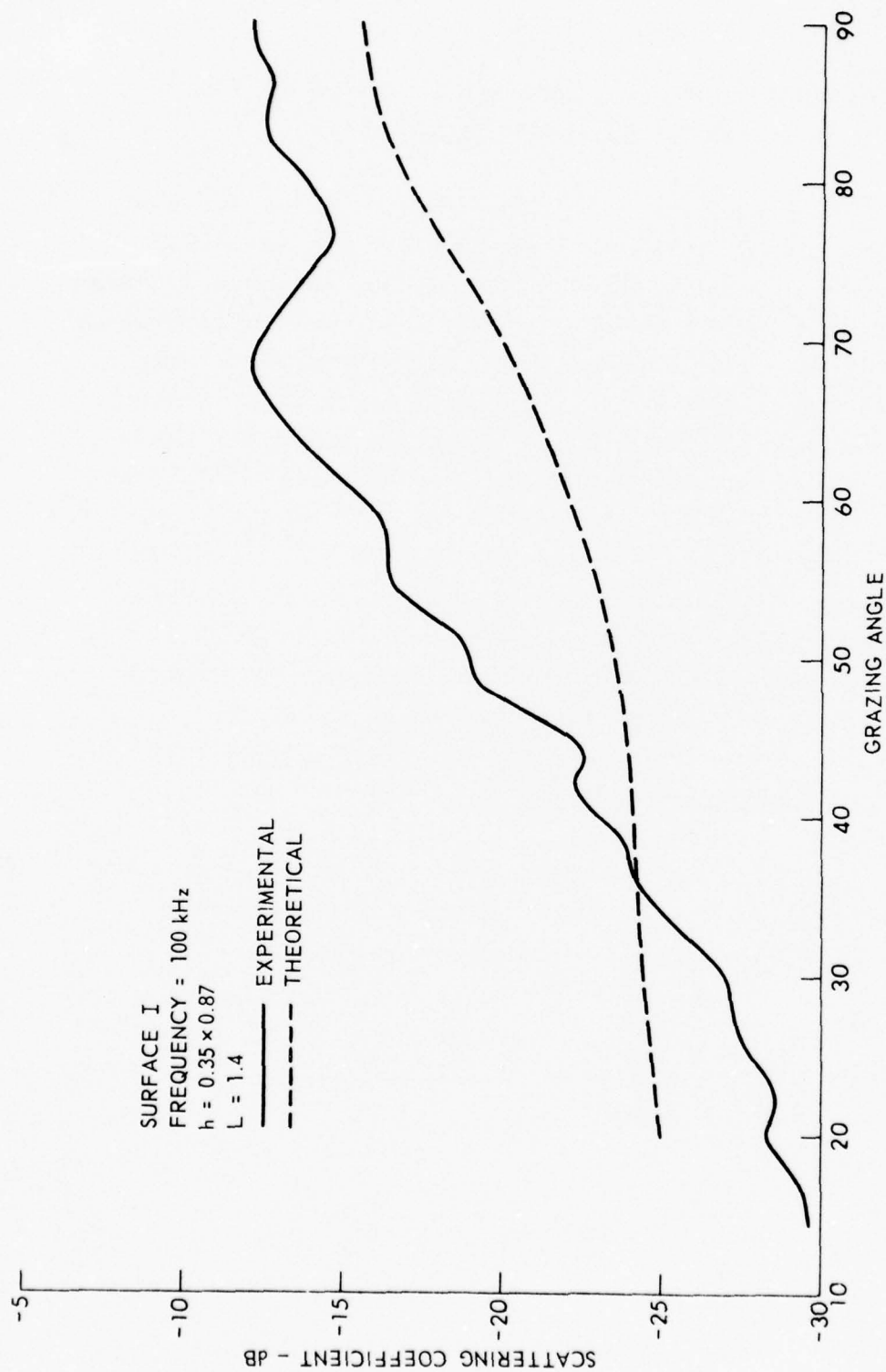
in deriving their results. As recently shown by Barrick [Ref. 4], the use of the exponential correlation is incorrect.

Since programming difficulties have occurred in the evaluation of Eq. (43), only Eq. (42) will be compared with the experimental data. Drawings AS-70-1174 and AS-70-1175 are two comparisons of theory with experiment. There are two ways these predictions can be improved: (1) by using the full series form of Eq. (43) instead of just the asymptotic form given by Eq. (42), and (2) by a more accurate evaluation of the slope correction term F. The expression for F given in this report is only the evaluation of the true slope correction term $(-\sin\theta_2 + \xi_x \cos\theta_2)$ at the stationary phase point $\xi_x = -V_x/V_z$. The resulting form for F is then taken out of the scattering integral. A much more accurate way to predict backscattered results would be to keep everything under the integral. When the above corrections are included in the form for the backscatter coefficient, the comparison of theory with experiment should be improved.

C. Fresnel High Frequency Backscatter

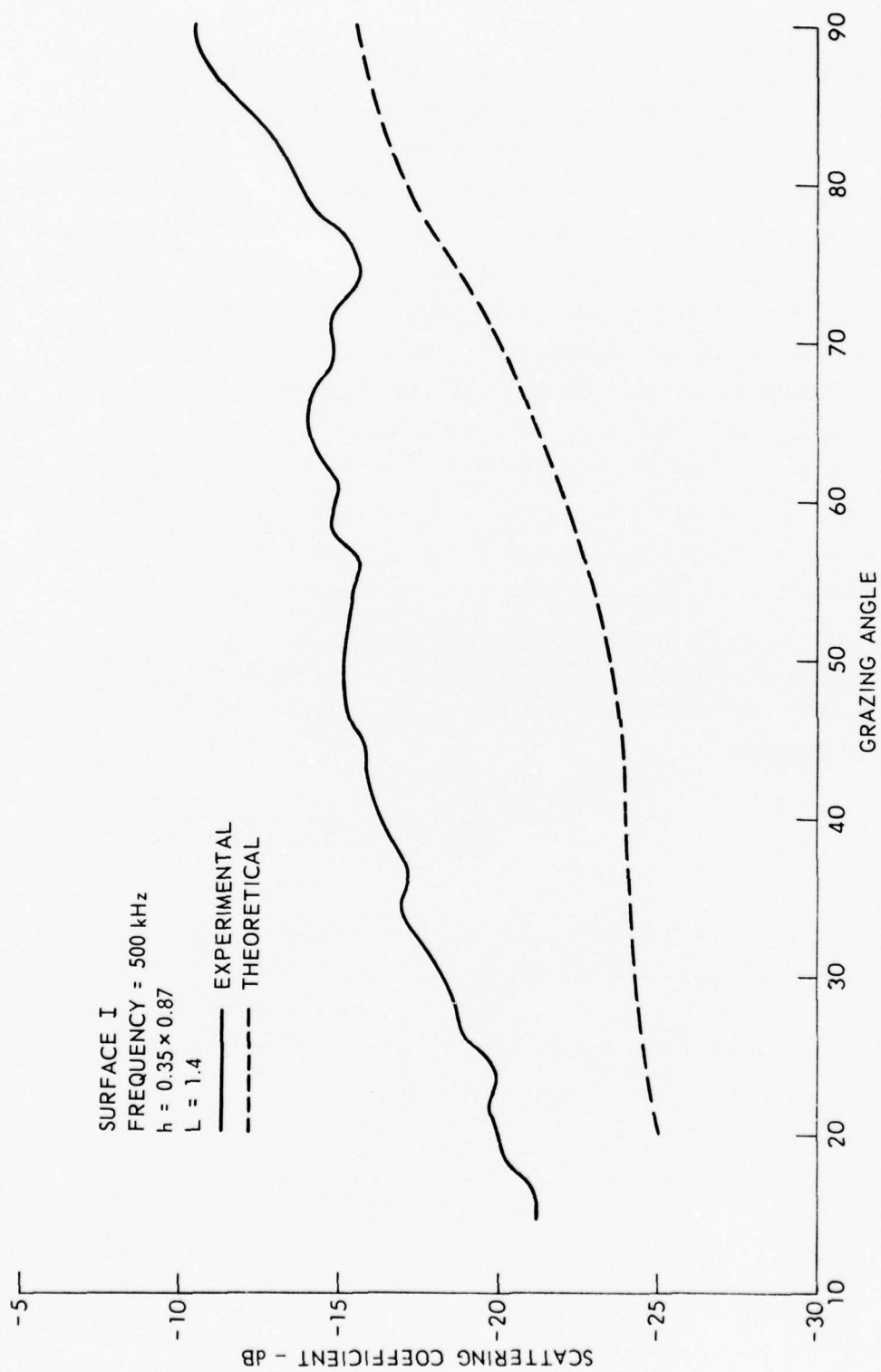
The intensity equation from which the high frequency backscatter predictions will be made was derived in the Final Report under Contract N00024-69-C-1275 and has the following form:

$$\begin{aligned} \langle I_s \rangle = & \left(\frac{k}{2\pi} \right)^2 \iiint \iiint_{\Sigma\Sigma'} P'_0 P_0 \frac{e^{+ik[(R_0 - R'_0) + (R_1 - R'_1)]}}{R_0 R'_0 R_1 R'_1} \\ & \times \left\langle e^{-ik\gamma(\xi - \xi')} \left[\left(\xi_x \hat{e}_x + \xi_y \hat{e}_y + \hat{e}_z \right) \cdot \hat{e}_1 \right] \right. \\ & \left. \times \left[\left(\xi'_x \hat{e}_x + \xi'_y \hat{e}_y + \hat{e}_z \right) \cdot \hat{e}_1 \right] \right\rangle dx dy dx' dy' \end{aligned} \quad (45)$$



BACKSCATTERING COEFFICIENT AS A FUNCTION OF GRAZING ANGLE

ARL - UT
 AS - 70 - 1174
 RLD - EJW
 10 - 1 - 70



BACKSCATTERING COEFFICIENT AS A FUNCTION OF GRAZING ANGLE

If the amplitude factor is disregarded, then P_0 is simply the directivity pattern of the source. In the final report mentioned previously and in the previous progress report under this contract, the necessity of using a directivity pattern and the Fresnel phase approximation was discussed. Also, an analytically tractable approximation for the directivity pattern was presented. The detailed results for the intensity calculation based on the assumption of Gaussian surface statistics were presented in the Final Report under Contract N00024-69-C-1275. However, at that time only the forward scatter results were presented. It was clear then that Gaussian statistics were inadequate for backscatter prediction since they do not predict the Lambert's Law type behavior, which occurs at small grazing angles; consequently, an investigation of other types of probability distributions of heights was undertaken.

Consider first how the stochastic nature of the problem is taken into account. The principal quantity of interest in Eq. (45) is the bracketed expression

$$\left\langle e^{-iky(\zeta-\zeta')} \left[(\zeta_x \hat{e}_x + \zeta_y \hat{e}_y - \hat{e}_z) \cdot \hat{e}_1 \right] \left[(\zeta'_x \hat{e}'_x + \zeta'_y \hat{e}'_y - \hat{e}'_z) \cdot \hat{e}'_1 \right] \right\rangle. \quad (46)$$

If the processes ζ and ζ' are assumed to be homogeneous and the following conventional approximations are made,

$$\hat{e}_x \cdot \hat{e}_1 = 0, \quad \hat{e}_y \cdot \hat{e}_1 = \cos \theta_r, \quad \hat{e}_z \cdot \hat{e}_1 = \sin \theta_r, \quad \gamma = \sin \theta_r + \sin \theta_i, \quad (47)$$

then according to Appendix B of the Final Report under Contract N00024-69-C-1275, Eq. (46) has the equivalent expression

$$\begin{aligned} \langle e^{-ik\gamma(\zeta-\zeta')} [\zeta] [\zeta'] \rangle &= \sin^2 \theta_r \langle \rangle + \frac{i \sin \theta_r \cos \theta_r}{k\gamma} \left(\frac{\partial}{\partial x} - \frac{\partial}{\partial x'} \right) \langle \rangle \\ &+ \frac{\cos^2 \theta_r}{k^2 \gamma^2} \frac{\partial^2}{\partial x \partial x'} \langle \rangle, \end{aligned} \quad (48)$$

where $\langle \rangle$ is a natural notation for $\langle e^{-ik\gamma(\zeta-\zeta')} \rangle$. In actually performing the derivatives indicated in Eq. (48), it will be assumed that the processes ζ and ζ' are also stationary; this implies $\partial h / \partial x_1 = 0$, where h is the rms value of the surface height. In addition, for a stationary process the correlation function depends only on the difference of the coordinates $\xi = x-x'$ and $\eta = y-y'$, resulting in a considerably easier integration.

The most interesting feature of Eq. (48) is that only knowledge of the characteristic function and the correlation function is needed to determine the quantities in Eq. (46) completely. That is, the probability distribution function that is required is $\omega(\zeta, \zeta')$, and not $\omega(\zeta, \zeta', \zeta_x, \zeta'_x, \zeta_y, \zeta'_y)$; as a result, the problem is much simpler.

The correlation functions that will be of interest in this progress report are the following:

$$\text{GAUSSIAN: } C(\xi, \eta) = e^{-\frac{\xi^2 + \eta^2}{L^2}} \quad (49)$$

$$\text{EXPONENTIAL: } C(\xi, \eta) = e^{-\frac{\sqrt{\xi^2 + \eta^2}}{L}} \quad (50)$$

and

$$\text{HAWKER: } C(\xi, \eta) = \frac{L^2}{L^2 + \xi^2 + \eta^2} \quad (51)$$

It was pointed out in Section B that the exponential correlation suffers from several disadvantages, most notably a lack of analyticity. In view of this problem, a search was made for a function which would behave like an exponential function moderately near the origin, and yet still be an analytic function; the resulting function we have named the Hawker correlation function. Therefore, in the actual calculation of backscattering, only the Gaussian and the Hawker correlation functions will be used.

It has previously been shown that the high frequency limits (or asymptotic forms) of the intensity are obtained by expanding the correlation function in series and retaining only the first two terms. Thus, for the Gaussian and Hawker correlation functions the high frequency limits are obtained respectively from

$$C(\xi, \eta)_G = 1 - \frac{\xi^2 + \eta^2}{L^2} + \dots \quad (52)$$

$$C(\xi, \eta)_H = 1 - \frac{\xi^2 + \eta^2}{L^2} + \dots \quad (53)$$

So that no confusion results, it is necessary to keep in mind that the parameter L , which is the correlation length, takes on different values in the Gaussian and Hawker correlation functions.

In addition to the two correlation functions, three different bivariate statistics will also be considered: Gaussian, Exponential, and Three-halves (Student's t with 3 degrees of freedom). The details of the characteristic function calculations were presented in Appendix A of the Final Report under N00024-69-C-1275, so they will be dispensed with here. In fact, most analytical details in the following calculations will be omitted so that only the final results will appear.

1. Gaussian Bivariate Distribution

The characteristic function for the Gaussian bivariate distribution is

$$\langle e^{-ik\gamma(\xi-\xi')} \rangle = e^{-g(1-C)} \quad (54)$$

Upon substitution of Eq. (52) in (54), one obtains

$$\langle \rangle^{h.f.} = e^{-\frac{g}{L^2}(\xi^2 + \eta^2)} \quad (55)$$

where $g = 4 \sin^2 \theta_r k^2 h^2$. When Eq. (55) is used in conjunction with Eq. (48), the Fresnel phase approximation, and beam function approximation in Eq. (45), the following result is obtained:

$$\langle I_s \rangle_{GAUSSIAN}^{h.f.} = G \left\{ \frac{1}{s^2} + \frac{4 \cot^2 \theta_r}{s^2} - \frac{\cot^2 \theta_r}{4} + \frac{\cot^4 \theta_r}{16 s^2} \right\} e^{-\frac{\cot^2 \theta_r}{s^2}} \quad (56)$$

where s is the rms slope and is given by

$$s = \frac{h\sqrt{2}}{L} \quad (57)$$

and

$$G = \frac{A}{16\pi K r_{10}^2 r_{00}^2} \quad (58)$$

Here A is the insonified elliptical area, and K is a constant related to the beam function. This result will be discussed in conjunction with the results for the other bivariate distributions.

2. Exponential Bivariate Distribution

The characteristic function for the Exponential bivariate distribution is

$$\langle e^{-ik\gamma(\xi-\xi')} \rangle = \frac{1}{[1 + \frac{2g}{3}(1-C)]^{3/2}}, \quad (59)$$

which becomes upon substitution of Eq. (49),

$$\langle \rangle^{h.f.} = \frac{1}{\left[1 + \frac{2g}{3L^2} (\xi^2 + \eta^2)\right]^{3/2}}. \quad (60)$$

Using Eq. (60), the backscattered intensity is obtained in a manner identical to the Gaussian calculation.

$$\begin{aligned} \langle I_s \rangle_{\text{EXPONENTIAL}}^{h.f.} &= G \left\{ \frac{3}{s^2} + \frac{6 \cot^2 \theta}{s^2} r - \cot^2 \theta_r - \frac{\sqrt{3} \cot^3 \theta}{s} r + \frac{3 \cot^4 \theta}{s^2} r \right\} \\ &\quad \cdot e^{-\frac{\sqrt{3} \cot \theta}{s} r}, \end{aligned} \quad (61)$$

where s and G are given by Eqs. (57) and (58).

3. Three-halves Bivariate Distribution

The high frequency version of the characteristics function for the Three-halves bivariate distribution is

$$\langle \rangle^{\text{h.f.}} = e^{-\sqrt{\frac{2g}{L^2}} (\xi^2 + \eta^2)} , \quad (62)$$

and from this the backscattered intensity is obtained as

$$\langle I \rangle_{3/2}^{\text{h.f.}} = G \left\{ \frac{1}{s^2} + \frac{2 \cot^2 \theta}{s^2} r + \frac{\cot^4 \theta}{s^2} r \right\} \cdot \frac{1}{\left[1 + \frac{\cot^2 \theta}{s^2} r \right]^{3/2}} . \quad (63)$$

It should be noted that the calculations leading to the intensities given by Eqs. (56), (61), and (63) were performed with the Gaussian correlation function. Comparison in Eqs. (52) and (53) shows that

$$L_G \leftrightarrow L_H . \quad (64)$$

Hence all of the results for the intensity calculated for the Gaussian correlation function can be extended to the Hawker correlation function by using the simple substitution given by Eq. (64). The values of L_G and L_H that give the best theoretical fits to the experimentally measured correlation function are 1.40 in. and 1.14 in., respectively. The slopes in each of the cases then become

$$s_G = \frac{h\sqrt{2}}{1.4} = h , \quad (65)$$

and

$$s_H = \frac{h\sqrt{2}}{1.14} = 1.24h . \quad (66)$$

Comparing Eqs. (64) and (65), it appears that in the high frequency limit a surface characterized by a Hawker correlation function behaves as a rougher surface than one characterized by a Gaussian correlation function because of the greater rms slope ($s_H > s_G$). This is an interesting feature since in the low frequency limit, the opposite is true because the Hawker function has much greater correlation than the Gaussian function in the tail.

In addition to the functional similarity obtained when using either a Hawker or a Gaussian correlation function, there are several other interesting features inherent in the high frequency limit. First notice that there is absolutely no frequency dependence in the intensities given by Eqs. (56), (61), and (63). Next, notice that there is no height dependence; rather the roughness dependence is based strictly on the rms slopes. Finally, it is clear from the parameter G that the intensity is area dependent and that the range dependence is given by $1/r_{10}r_{00}$ and not by geometrical acoustics, i.e., $1/(r_{10}+r_{00})$. In previous reports, it has been shown that for planar surfaces the geometrical acoustics range dependence $1/(r_{10}+r_{00})$ is obtained as predicted by image theory, and there is no insonified area dependence for an infinite plane. Also, in the Final Report under Contract N00024-69-C-1275 it was noted that for moderately rough surfaces at medium frequencies the range dependence was quasi-geometrical acoustics, and there was little area dependence. Thus, in passing to the high frequency limit, the Fraunhofer range dependence, which has been characteristic of all other theories, is clearly obtained. However, there must obviously be some transition region which none of the other theories have taken into account. It has been claimed in some papers that even in the low frequency limit (Eckart, for example) the Fraunhofer range dependence is obtained.

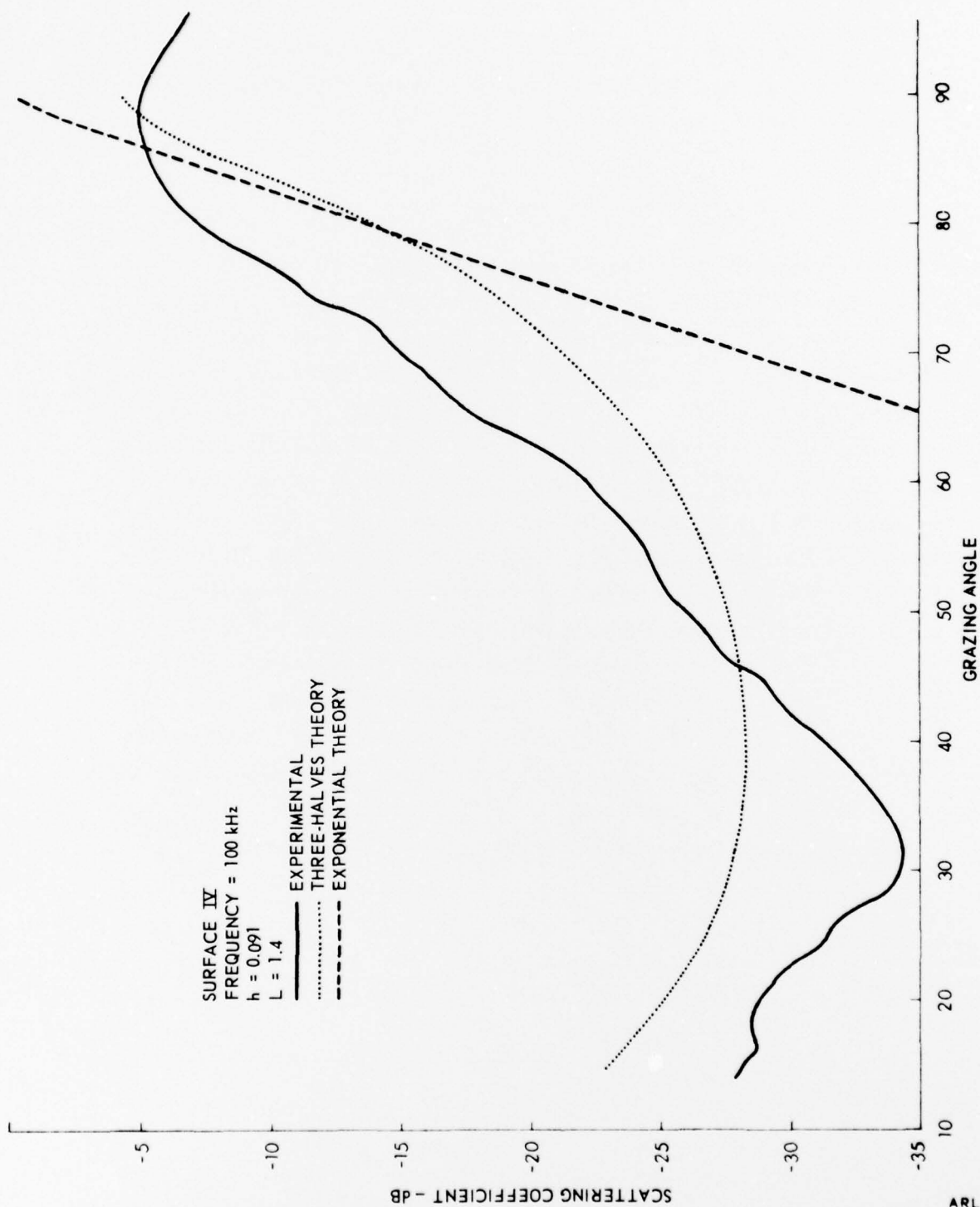
The theoretical and experimental quantities compared in Dwgs. AS-70-1194, AS-70-1195, and AS-70-1196 are the scattering coefficients defined by Eq. (36):

$$\sigma = \langle I_s \rangle (r_{10} + r_{00})^2, \quad (67)$$

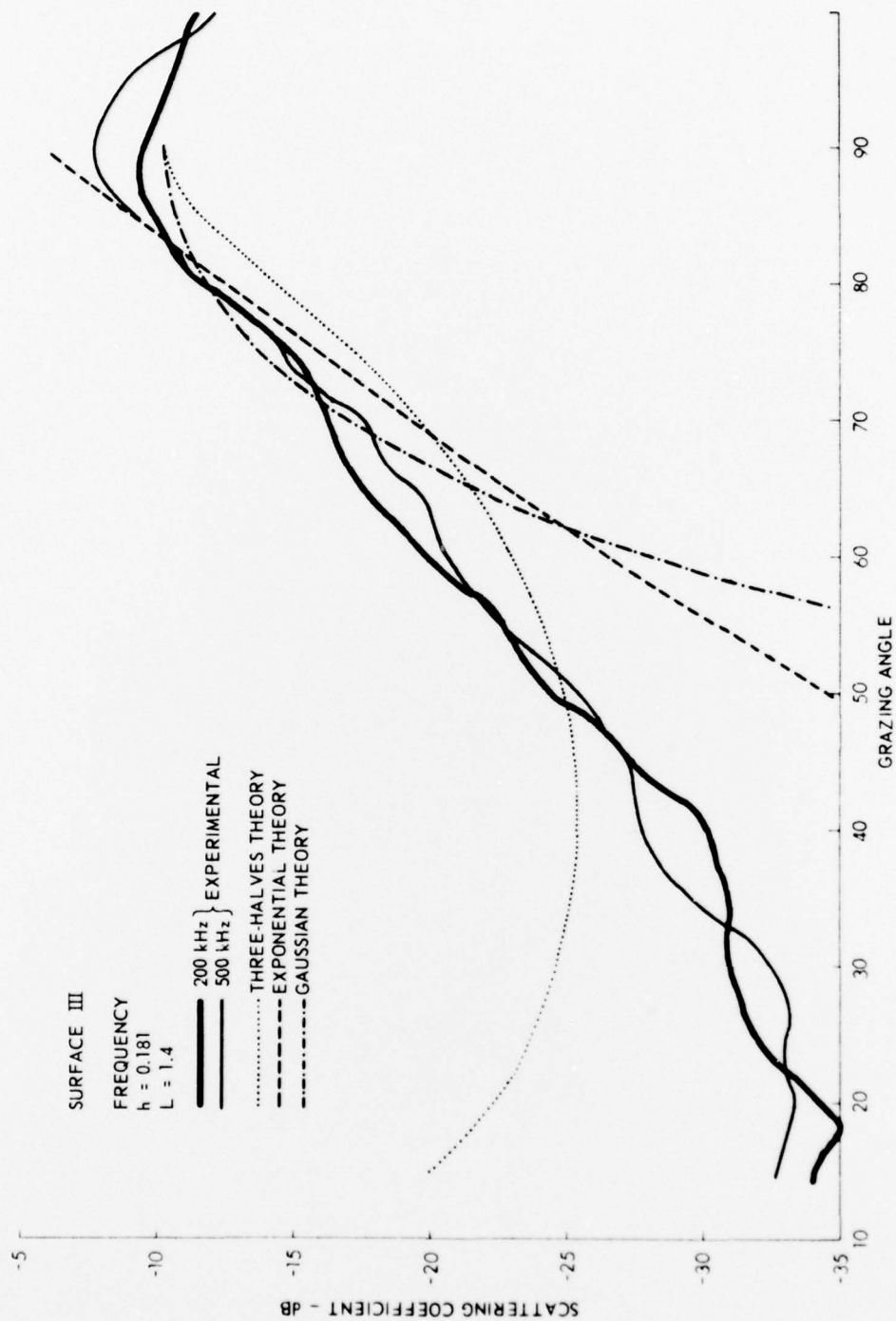
where the theoretical backscattered intensities given by Eqs. (56), (61), and (63) have been used. Care was taken in the selection of the experimental data to be sure that they actually corresponded to the high frequency limit. It is fairly certain that the data shown for surfaces III and I are in the high frequency limit, since the 200 kHz and 500 kHz lie quite close together; that is, they exhibit no frequency dependence. Another interesting aspect of the drawings is the notable lack of agreement between experiment and the theoretical predictions. This was unexpected since the Three-halves and Exponential distributions resulted in extremely good agreement between experiment and theory for the coherent intensity and for the forward scattered intensity. One of the most prominent aspects of the Three-halves theory is the upturn in the predicted backscattered intensity at grazing angles below 40 deg. If shadowing theory had been incorporated, this feature would not be so pronounced even though it would still be present. The reason for this behavior is that at low angles the Three-halves distribution predicts that the major intensity component will be given by

$$\frac{\cot^4 \theta_r}{s^2 \left[1 + \frac{\cot^2 \theta_r}{s^2} \right]^{3/2}} \approx s \cot \theta_r. \quad (68)$$

This type of dependence at low grazing angles is due strictly to the inclusion of slope correction terms in the intensity integrals.

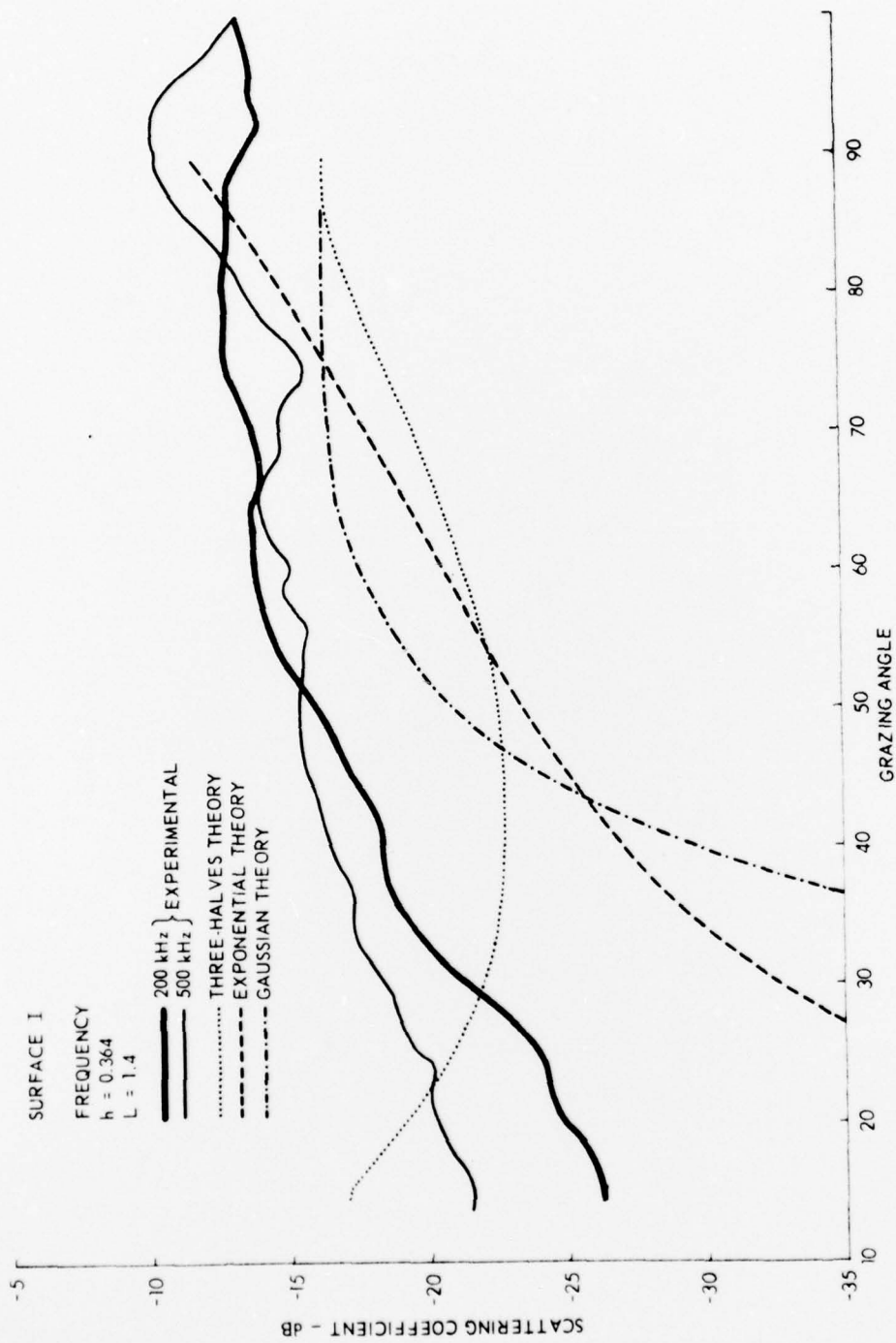


BACKSCATTERING COEFFICIENT AS A FUNCTION OF GRAZING ANGLE



BACKSCATTERING COEFFICIENT AS A FUNCTION OF GRAZING ANGLE

ARL - UT
 AS - 70 - 1195
 PJW - ORS
 10 - 13 - 70



BACKSCATTERING COEFFICIENT AS A FUNCTION OF GRAZING ANGLE

ARL - UT
 AS-70-1196
 PJW - ORS
 10-13-70

Examination of the stationary phase backscattered intensity expression [Eq. (42)] does not reveal a similar difficulty since the slope was evaluated at the stationary phase point in Eq. (42).

Because of the lack of agreement in the theoretical and experimental backscattering expressions, additional aspects on the backscattering problem will have to be examined. In the next section, for example, a qualitative investigation of composite surface scattering will be given. Also, it is hoped that in the next progress report the integrations of certain other promising bivariate distributions will be completed, and some results for composite surfaces will be available.

D. Composite Surface Theory

Recently there have been several attempts to explain backscattering effects by using the composite surface model. However, as pointed out in the introduction, these attempts have not given physically consistent predictions for both backward and forward scattering. In this section, qualitative arguments will be developed which show that the composite nature of the surface can have a significant effect only on the backscattered portion of the intensity. The small scale roughness does not significantly affect the specular or the forward scattered intensity.

Assume the random surface process is represented by

$$\zeta(x,y) = \zeta_1(x,y) + \zeta_2(x,y) \quad , \quad (69)$$

where ζ_1 and ζ_2 are independent stationary random functions with zero mean, each with its own statistical distribution and correlation

function. In addition, the processes are such that the rms values of the heights obey:

$$h_1 \gg h_2, \text{ and } \lambda > h_1 \quad . \quad (70)$$

Equation (70) merely implies that ζ_1 represents some large scale roughness while ζ_2 represents some small scale roughness. Here λ is the source wavelength, which must be about the same order of magnitude or greater than h_1 .

Recall that for the pressure, the statistical quantity of interest is given by

$$\left\langle \left[\sin\theta_r - (\eta_1 + \eta_2) \cos\theta_r \right] \cdot \left(e^{-ik\gamma(\zeta_1 + \zeta_2)} \right) \right\rangle , \quad (71)$$

where η_i is defined as $\partial\zeta_i/\partial y$ and is independent of ζ_i . Based on this independence, Eq. (71) can be written as

$$\sin\theta_r \langle \rangle - \cos\theta_r \left(\langle \eta_1 \rangle + \langle \eta_2 \rangle \right) \langle \rangle , \quad (72)$$

where $\langle \rangle$ represents $\left\langle e^{-ik\gamma(\zeta_1 + \zeta_2)} \right\rangle$ and again the brackets mean the stochastic average. If it is assumed that ζ_1 and ζ_2 are distributed in the same manner, then essentially

$$\langle \rangle = X \left[k^2 \gamma^2 (h_1^2 + h_2^2) \right] , \quad (73)$$

where X is the general notation for the characteristic function.

However, from Eq. (70), one sees that

$$\langle \rangle = x[k^2 \gamma^2 (h_1^2 + h_2^2)] \approx x[k^2 \gamma^2 h_1^2] \quad (74)$$

Clearly, the small scale roughness is insignificant in the characteristic function.

Now examine the averages η_1 and η_2 . If shadowing is ignored, then since ξ_1 and ξ_2 were zero mean random processes, it is known that η_1 and η_2 are also zero mean random processes if ξ_1 and ξ_2 are homogeneous. However, some very crude shadowing approximations can be made. First recall that η is the tangent to the surface at the point (x,y) on the surface. Then if the possibility of the point (x,y) on the surface being shadowed by some other near lying surface point is ignored, it can be claimed that the point is not shadowed if

$$-\tan\theta_i < \eta < \tan\theta_r \quad (75)$$

Hence the averages of η_1 and η_2 are not given by

$$\langle \eta_i \rangle = \int_{-\infty}^{\infty} \eta_i \omega(\eta_i) d\eta_i \quad , \quad (76)$$

but rather by

$$\langle \eta_i \rangle = \int_{-\tan\theta_r}^{\tan\theta_r} \eta_i \omega(\eta_i) d\eta_i \quad , \quad (77)$$

since only those values of η_i that are not shadowed with respect to both the source and receiver can contribute to the pressure integral.

In Eqs. (76) and (77), $\omega(\eta_i)$ is the probability distribution of η_i and will be required to be an even, zero mean function. With this in mind, various cases of Eq. (77) can now be investigated. In the specular direction $\tan\theta_i = \tan\theta_r$, then $\langle\eta_1\rangle$ and $\langle\eta_2\rangle$ equal zero from Eq. (77). Also, in forward scatter $\tan\theta_i$ does not differ appreciably from $\tan\theta_r$ for most cases, and again $\langle\eta_1\rangle$ and $\langle\eta_2\rangle$ are essentially zero. However, for backscattering $\tan\theta_i \rightarrow \infty$, and, depending on the value of $\tan\theta_r$, the averages can differ appreciably from zero. For normal incidence, $\tan\theta_r \rightarrow \infty$, and again $\langle\eta_1\rangle$ and $\langle\eta_2\rangle$ are zero, but as the grazing angle approaches zero, Eq. (77) becomes

$$\langle\eta_i\rangle = - \int_0^{\infty} \eta_i \omega(\eta_i) d\eta_i \quad . \quad (78)$$

This is the case where $\langle\eta_1\rangle$ and $\langle\eta_2\rangle$ take on their greatest value. Suppose that while the rms value of the heights of the large scale roughness satisfies $h_1 \gg h_2$ as can often be the case, the rms value of the slopes of the small scale roughness, s_2 , satisfies $s_2 \gg s_1$. Then $\langle\eta_2\rangle \cong \langle\eta_1\rangle$, and if $h_1 \gg h_2$, then Eq. (72) becomes

$$\sin\theta_r \chi[k^2 \gamma^2 h_1^2] + \cos\theta_r \langle\eta_2\rangle \chi[k^2 \gamma^2 h_1^2] \quad . \quad (79)$$

A good physical example of a composite process where this would be true would be sand dunes made up of angular grains of sand. The heights of the dunes would be very much greater than the grain sizes, but the slopes of the angular faces of the grains can be very much greater than the slopes of the dunes. A realistic example of scattering by this type of composite surface is the scattering of light by seemingly flat snow fields.

Examination of Eq. (79) reveals the very interesting behavior that can be exhibited by certain types of composite surfaces. For most forward and for all specular scattering, the lead term, which depends only on the large scale roughness, dominates. Also, for backscattering at near normal incidence, the lead term dominates; that is, the large scale roughness is again the major factor. However, for backscattering at low grazing angles the second term in Eq. (74) is predominant. Hence, it is only at low grazing angle backscatter that the small scale roughness can contribute and only then if it has an appreciable rms slope value.

Let us summarize the preceding arguments. For a composite surface model to be useful the following conditions must be met:

$$h_1 \gg h_2 \quad ,$$

$$\lambda > h_1 \quad ,$$

$$s_2 \gg s_1 \quad .$$

The second condition merely implies that the high frequency limit must not have been reached since the scattered intensity is then strictly slope dependent, and the small scale roughness will dominate the scattering effects at all angles. Finally, for physically consistent results to be obtained for both forward- and backscattering, shadowing considerations must be employed.

REFERENCES

1. A. K. Fung and A. Leovaris, "Experimental Verification of the Proper Kirchhoff Theory of Wave Scattering from Known Randomly Rough Surfaces," J. Acoust. Soc. Am. 46, 1057-1061 (1969).
2. P. Beckmann, "Radar Backscatter from the Surface of the Moon," J. Geophys. Res. 70, 2345-2350 (1965).
3. A. H. Marcus, "Application of a Statistical Surface Model to Planetary Radar Astronomy," J. Geophys. Res. 74, 4958-4962 (1969).
4. D. E. Barrick, "Unacceptable Height Correlation Coefficients and the Quasi-Specular Component in Rough Surface Scattering," Radio Sci. 5, 647-654 (1970).

8 October 1970

DISTRIBUTION LIST FOR
QUARTERLY PROGRESS REPORT UNDER CONTRACT N00024-70-C-1279
FOR THE PERIOD 1 JULY - 30 SEPTEMBER 1970
UNCLASSIFIED, FOR OFFICIAL USE ONLY

Copy No.

	Commander Naval Ship Systems Command Department of the Navy Washington, D. C. 20360
1	Attn: SHIPS OOV1L
2	Attn: PMS-387
3	Commander Naval Undersea Research and Development Center San Diego Division 271 Catalina Boulevard San Diego, California 92152 Attn: Code 503
	Director U. S. Naval Research Laboratory Department of the Navy Washington, D. C. 20390
4	Attn: Code 8120
5	Attn: Code 8172
6 - 7	Officer-in-Charge New London Laboratory Naval Underwater Systems Center New London, Connecticut 06320 Attn: Code 2211
	Commanding Officer and Director U. S. Naval Ship Research and Development Laboratory Panama City, Florida 32402
8	Attn: Code 700
9	Attn: Code 720

Distribution List for QPR, under Contract N00024-70-C-1279
for the period 1 July - 30 September 1970

Copy No.

- | | |
|---------|---|
| 10 | Superintendent
U. S. Naval Postgraduate School
Monterey, California 93940
Attn: Prof. H. Medwin |
| 11 | Office of Naval Research
Resident Representative
Lowich Building
1103 Guadalupe
Austin, Texas 78701 |
| 12 | G. R. Barnard, ARL/UT |
| 13 | M. L. Boyd, ARL/UT |
| 14 | R. L. Deavenport, ARL/UT |
| 15 | H. G. Frey, ARL/UT |
| 16 | P. J. Welton, ARL/UT |
| 17 | Library, ARL/UT |
| 18 - 19 | ARL Reserve |

UNCLASSIFIED,
Security Classification

DOCUMENT CONTROL DATA - R & D		
Security classification of title, body of abstract and indexing annotation must be entered when the overall report is classified.		
1. ORIGINATING ACTIVITY (Corporate author)		2a. REPORT SECURITY CLASSIFICATION
Applied Research Laboratories The University of Texas at Austin Austin, Texas 78712		UNCLASSIFIED,
2. REPORT TITLE		2b. GROUP
QUARTERLY PROGRESS REPORT UNDER CONTRACT N00024-70-C-1279		---
4. DESCRIPTIVE NOTES (Type of report and inclusive dates)		
Progress Report for the period 1 July - 30 September 1970		
7. AUTHOR(S) (First name, middle initial, last name)		

11. REPORT DATE		
8 October 1970		
7b. TOTAL NO OF PAGES		
42		
7c. NO OF REFS		
4		
5a. CONTRACT OR GRANT NO		9a. ORIGINATOR'S REPORT NUMBER(S)
N00024-70-C-1279		---
5. PROJECT NO		9b. OTHER REPORT NO(S) (Any other numbers that may be assigned this report)
SF 11552-001, Task 8118		---
10. DISTRIBUTION STATEMENT		
Each transmission of this document outside the Department of Defense must have prior approval of SHIPS COVIL.		
11. SUPPLEMENTARY NOTES		12. SPONSORING MILITARY ACTIVITY
---		Naval Ship Systems Command Department of the Navy (NAVSEA 06H1-4) Washington, D. C. 20360
13. ABSTRACT		
<p>In Section I the Rayleigh reflection coefficient for a rough surface is derived in a form suitable for inclusion in the basic integral for the scattered pressure. A formula for the pressure scattered from a rough attenuating surface is then derived using this coefficient. The backscattered intensity is calculated in Section II for various assumed distributions of surface heights. The results presented here are restricted to the high frequency limit, and are developed using both the stationary phase and the modified Fresnel techniques. Finally, a backscattering result for a composite surface is derived, and is shown to be consistent for both forward and backward scattering. (U-)</p>		

APPLIED
RESEARCH
LABORATORIES
THE UNIVERSITY OF TEXAS
AT AUSTIN

